PACS: 12.10Kt, 23.20.En,24.10.-i, 25.40.Lw, 25.70.Gh

ROLE OF ANGULAR MOMENTUMUM IN CAPTURE OF HEAVY NUCLEI

R.A. Anokhin, K.V. Pavlii
National Science Center "Kharkov Institute of Physics and Technology"
Akademicheskaya 1, 61108, Kharkov, Ukraine
E-mail: kvint@kipt.kharkov.ua
Received January 31, 2013, accepted February 21, 2013

The influence of angular momentum on the dynamics of the heavy nucleus interaction in the capture process is analyzed on a dynamic-statistical approach. The range of light nuclei and stability region for angular momentum, where capture is possible, are determined on the basis of analysis of the nucleus-nucleus potential for reactions with heavy nuclei $^{238}_{92}$U, $^{244}_{94}$Pu, $^{248}_{96}$Cm and $^{251}_{98}$Cf. The capture cross sections of compound nuclei with $Z_0 = 120$ and 126 are calculated, and the most perspective reactions to obtain the superheavy elements are pointed out.
KEY WORDS: angular momentum, synthesis of superheavy elements, stability region, capture cross section.

РОЛЬ УГЛОВОГО МОМЕНТА В ПРОЦЕССЕ ЗАХВАТА ТЯЖЕЛЫХ ЯДЕР
Р.А. Анохин, К.В. Павлий
Национальный научный центр «Харьковский физико-технический институт»
ул. Академическая, 1, 61108, г. Харьков, Украина
На основании динамико-статистического описания рассматривается влияние углового момента на динамику взаимодействия тяжелых ядер в процессе захвата. Диапазон легких ядер и область стабильности углового момента где возможен захват определены при анализе ядро-ядерного потенциала для реакций с тяжелыми ядрами $^{238}_{92}$U, $^{244}_{94}$Pu, $^{248}_{96}$Cm и $^{251}_{98}$Cf. Было рассчитано сечение захвата для составных ядер с $Z_0 = 120$ и 126 и определены наиболее перспективные реакции для получения сверхтяжелых элементов.
КЛЮЧЕВЫЕ СЛОВА: угловой момент, синтез сверхтяжелых элементов, область стабильности, сечение захвата.

РОЛЬ КУТОВОГО МОМЕНТУ В ПРОЦЕСІ ЗАХВАТУ ВАЖКИХ ЯДЕР
Р.О. Анохін, К.В. Павлій
Національний науковий центр «Харківський фізико-технічний інститут»
вул. Академічна, 1, 61108, м. Харків, Україна
Виходячи з динаміко-статистичного опису розглядається вплив кутового моменту на динаміку взаємодії важких ядер в процесі захвату. Діапазон легких ядер і область стабільності кутового моменту де можливий захват визначені при аналізі ядро-ядерного потенціалу для реакцій з важкими ядрами $^{238}_{92}$U, $^{244}_{94}$Pu, $^{248}_{96}$Cm і $^{251}_{98}$Cf. Було розраховано переріз захвату для складених ядер з $Z_0 = 120$ і 126 та визначено найбільш перспективні реакції для отримання надважких елементів.
КЛЮЧОВІ СЛОВА: кутовий момент, синтез надважких елементів, область стабільності, переріз захвату

"Cold" and "hot" fusion reactions are used in the experimental study of mechanisms of synthesis of new superheavy elements (SHE). Increase of the charge number of the heavy nucleus enables synthesizes of new elements with accelerators. SHE with $Z_0 = 112$ (charge number) and $Z_0 = 113-118$ [1-3] were obtained in the "cold" and "hot" fusion reactions respectively. The improvement of acceleration technology with increase of beam intensity is required in the course of SHE formation for the purpose of further promotion of experimental works on Z_0 scale, since the expected cross section of new SHE does not exceed several femtobarn [3]. In NSC KIPT acceleration structures are developed for the purpose of experimental study of heavy nuclei fusion characteristics [4, 5].

In the description of heavy nuclei fusion with fixed mass A_i and charge Z_i numbers ($i = 1, 2$) SHE formation cross section is calculated [6] as follows:

$$\sigma_{ER} = \sum_{L=0} \sigma_{cap}(E_{cm}, L) \cdot P_{CN}(E_{cm}, L) \cdot W_s(E_{cm}, L), \quad (1)$$

where $\sigma_{cap}(E_{cm}, L)$ – partial capture cross section of the incident nucleus capture by the target nucleus; $P_{CN}(E_{cm}, L)$ – probability of the compound nucleus formation after capture; $W_s(E_{cm}, L)$ – survivability of the compound nucleus with respect to fission, L – angular momentum, E_{cm} – light nucleus kinetic energy.

The aim of this article is to study influence of the angular momentum on the capture probability and cross section for perspective fusion reactions of heavy nuclei with $Z_0 = Z_1 + Z_2$ equal 120 and 126.

INTERACTION POTENTIAL AND DYNAMICS

The main process determining the capture cross section is the dynamics of interacting nuclei from the moment of contact to the minimum of the nucleus-nucleus potential (interaction potential). The kinetic energy of the beam, which is almost completely converted into the excitation energy, decreases during the change of distance between the nuclei centers; in addition, the angular momentum of the interacting nuclei is reduced leading to the change in the nucleus-nucleus potential.

Interaction potential

In describing dynamics of interacting nuclei, an important role is played by the choice of nucleus-nucleus potential, which is determined as follows: $V_{nn}(R,L) = V_{Coul}(R) + V_n(R) + V_{rot}(R,L)$. $V_{Coul}(R)$ – Coulomb potential which is calculated from the partial overlap of the nuclei volumes according to [7]. $V_n(R)$ – nuclear potential of short-range forces (proximity potential) which has almost no fitted parameters [8]. $V_{rot}(R,L)$ – centrifugal potential, where the expression for the solid momentum of inertia of the nuclear system is applied:

$$V_{rot}(R,L) = \frac{\hbar^2 L(L+1)}{2\mu R^2} \qquad (2)$$

where R – distance between the centers of nuclei, $\hbar$ – Planck constant, μ – reduced mass, and L – system angular momentum. Nucleus-nucleus potential allows to determine the following parameters influencing the dynamics: Coulomb barrier B_{Coul}, quasifission barrier B_{qf}^{R}, distance between the centers of nuclei at the touch, at the Coulomb barrier (maximum) and at the minimum of the nucleus-nucleus potential.

In determining capture cross section, according to [6], $B_{qf}^{R} > 0$ is required, i.e. the existence of potential pocket in the nucleus-nucleus potential is necessary, otherwise σ_{cap} will be equal to zero. Fig. 1 shows the dependence of the potential pocket depth ΔV_{nn} on the charge number of light nucleus for different isotopic configurations of light nuclei, with heavy nucleus – $^{248}_{96}Cm$. These calculations are made for heavy fragments $^{238}_{92}U$, $^{244}_{94}Pu$, $^{248}_{96}Cm$ and $^{251}_{98}Cf$, from which it follows that the depth of the potential pocket is deeper for more asymmetric reactions, while the capture cross section is higher [9]. With increasing the quantity of neutrons in the light nucleus, the depth of the potential pocket increases. Therefore, the choice of the target nuclei and the beam can be made in planning of experimental work on the accelerator. However, as the potential pocket depth is reduced, the probability of capture and, consequently, the capture cross section of the interacting nuclei decrease. Therefore, these characteristics are to be correctly calculated.

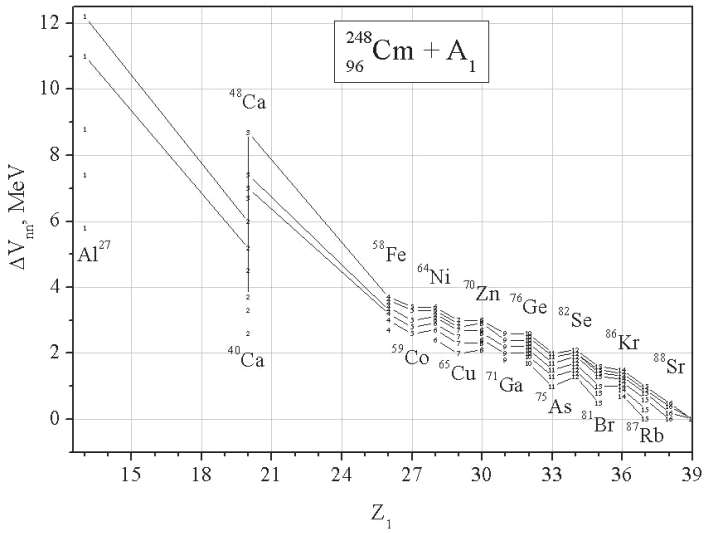

Fig. 1. Dependence of the potential pocket depth in the nucleus-nucleus potential on the charge number of light nucleus with different numbers of neutrons, heavy nucleus – $^{248}_{96}Cm$.

Dependencies of ΔV_{nn} on Z_1 (Fig. 1) are calculated at $L = L_0 = 0$. As a rule, a series of angular momenta, which contribute to the determination of the capture cross section, is involved in fusion reactions. A critical value of the angular momentum L_c exists; if $L > L_c$, then the capture is impossible and $\sigma_{cap}(L > L_c) = 0$. Fig. 2 shows the dependence of the interaction force ($\partial V_{nn} / \partial R = F_{nn}$) on the distance between the centers of nuclei at different values of the angular momentum.

As L increases, the potential pocket depth decreases and convergence of R_{min} and R_{max} (point of minimum and maximum values of V_{nn}) takes place; it corresponds to $F_{nn} = 0$ on the graph. When $L = L_c$, F_{nn} becomes less than

zero. Consequently, the stability region, in which the capture is possible, is determined for each reaction by L_c value (Fig. 3). The capture condition, from which L_c is derived, can be written as follows:

$$\frac{\partial V_{nn}}{\partial R} = \frac{\partial}{\partial R}(V_{Coul} + V_n + V_{rot}) \geq 0 . \quad (3)$$

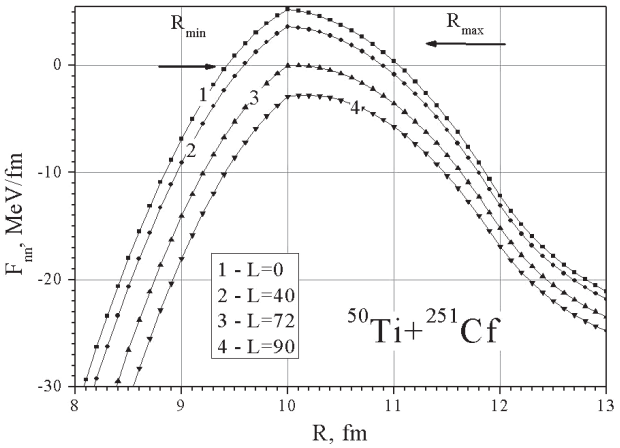

Fig. 2. Dependence of $\partial V_{nn} / \partial R = F_{nn}$ on the distance between the centers of nuclei at different values of the angular momentum.

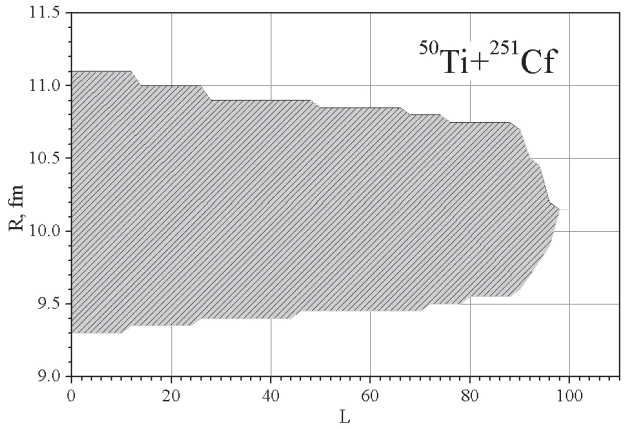

Fig. 3. Stability region depending on the angular momentum.

However, the angular momentum of the system at the point of capture depends on dynamic parameters, the influence of which cannot be disregarded, i.e. $L = L(t)$. For dynamic stability, when the angular momentum depends on the time, system of equations (4) is to be solved. Consequently, nuclei with different initial values of the angular momentum L_{0i} are involved in the fusion reactions; this should be considered within the nucleus-nucleus potential from the contact point to the momentum of capture.

In studies of the dynamics of interacting nuclei at the initial stage of formation of SHE (capture), the dynamics of change in the centrifugal potential and, therefore, of the angular momentum, as it makes a significant contribution to the capture cross section, and, thus, in the cross section of SHE formation, are to be taken into consideration.

Dynamics

For dynamic description of the interacting nuclei the following system of equations [7, 9] is used:

$$\begin{cases} \mu \dfrac{d\dot{R}(t)}{dt} + k_R \left(\dfrac{\partial V_n(R)}{\partial R} \right)^2 \dot{R}(t) = F_{nn}(R, L) \\ \mu \dfrac{dL(t)}{dt} + k_\theta \left(\dfrac{\partial V_n(R)}{\partial R} \right)^2 L(t) = 0 \end{cases}, \quad (4)$$

where $k_R = 1 \cdot 10^{-23}$ s/MeV and $k_\theta = 0.01 \cdot 10^{-23}$ s/MeV are radial and tangential friction coefficients respectively [9]. This system was numerically solved on the range of R from the contact point of interacting nuclei $R_{cont} = 1.28(A_1^{1/3} + A_2^{1/3})$ up to the momentum of capture, where the following condition is met:

$$\sqrt{\Delta E_{cm}} \cdot \Delta R \leq \frac{\hbar}{2 \cdot \sqrt{2\mu}} . \quad (5)$$

This condition is met in the minimum of the potential pocket of the nucleus-nucleus potential, when $E_{cm} \to 0$ (relative kinetic energy of interacting nuclei), and $R \to R_{min}$. In the solution of the system (4), the step was chosen by kinetic energy – 1 MeV, and by angular momentum 1. Fig. 4 shows the dependence of change in the kinetic energy on the distance between the nuclei centers for different initial values of the angular momentum. The figure shows that the system enters the capture channel after overcoming the Coulomb barrier R_{max}, with a sharp decrease of the kinetic energy (curves 1 – 4), for $0 \leq L_0 < 72$.

After overcoming the Coulomb barrier the system oscillates around the interaction potential minimum with decay of the amplitude of E_{cm}, due to dissipative forces, Fig. 4. Then, the condition (5) can be rewritten as follows:

$$\lim_{j\to\infty}\left(\frac{1}{j}\int_{R_2^{min}}^{R_1^{min}}\sqrt{E_{cm}(R)}dR\right)\le\frac{\hbar}{2\cdot\sqrt{2\mu}}, \qquad (6)$$

where j – number of steps in one oscillation. In the solution of system (4) and the evaluation of expression (6) $j\ge 70$; R_1^{min}, R_2^{min} – distance between the centers of interacting nuclei with $E_{cm}\to 0$ (see Fig. 5). The change in oscillation period was determined by the change of sign $\partial E_{cm}/\partial t$ from minus to plus. The integral in expression (6) was numerically calculated for each step according to Δt up to the change in the sign $\partial E_{cm}/\partial t$.

Step by time was chosen $(0.1\div 1)\cdot 10^{-23}$, while the average change in distance between the centers of interacting nuclei after the passage of the Coulomb barrier is equal to $\sim 10^{-4}$ fm, the stopping of calculations was performed under $\Delta E_{cm}\le 0.3\cdot 10^{-13}$ MeV according to the expression (6). Fig. 4 shows the curve 5 for $L_0=80$, the system does not overcome the Coulomb barrier and is disintegrated with the increase in the kinetic energy if $L_0\ge 80$. In this case the solution of system (4) was terminated under conditions where $R\ge R_{max}$. Consequently, the role of change in the angular momentum and thus the centrifugal potential are principal in the determination of the capture cross section.

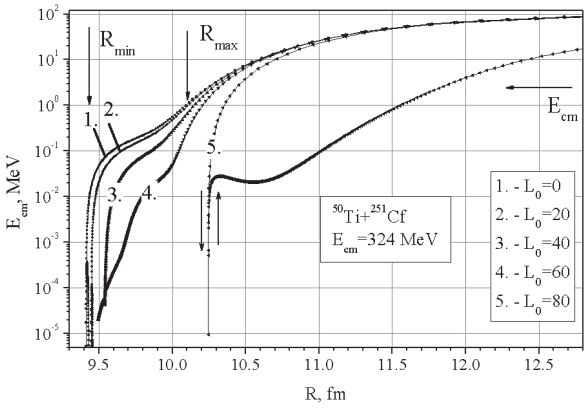

Fig. 4. Dependence of change in the kinetic energy on the distance between the centers of nuclei. Dynamics of the process is shown from right to left. The arrows indicate the regions of R_{max} maximum and R_{min} minimum values of the nucleus-nucleus potential.

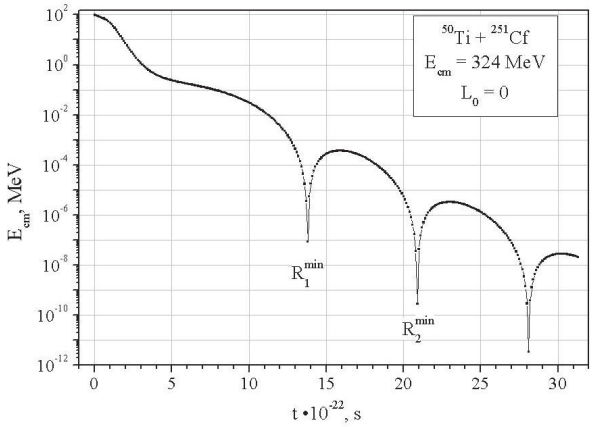

Fig. 5. Dependence of the kinetic energy on the time in the area of minimum of the nucleus-nucleus potential.

Fig. 6 shows the dependence of change in the centrifugal potential on the time required for reaction $^{50}Ti+{}^{251}Cf$ with different values of L_0.

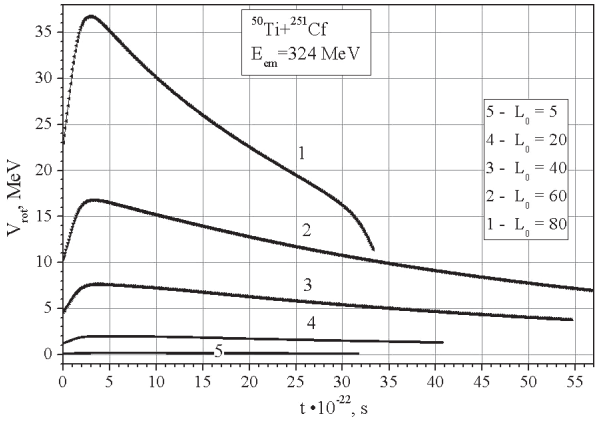

Fig. 6. Dependence of the centrifugal potential on the interaction time for reaction $^{50}Ti+{}^{251}Cf$. 1 – L_0=80, 2 – L_0=60, 3 – L_0=40, 4 – L_0=20, 5 – L_0=5.

The figure shows that at the initial instant the centrifugal potential increases due to the reduction of the distance between centers of nuclei. After overcoming the Coulomb barrier, V_{rot} is reduced due to more strong exponential dependence of the angular momentum on time and reduction of relative velocity of nuclei. This conclusion is supported by the fact that the change of $L(t)$ should be considered in the calculation of the capture cross section, since the change of the Coulomb barrier and the quasifission barrier leads to changes of energy, required for its overcoming, and, consequently, to change in the capture probability.

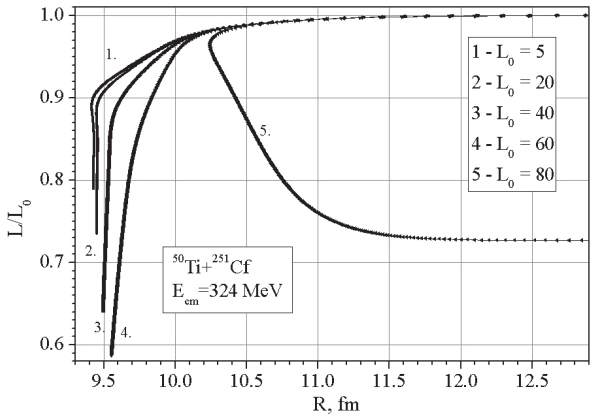

Fig. 7. Dependence of the reduced angular momentum on the relative distance between centers of nuclei.

Fig. 7 shows the dependence of the change in the relative angular momentum for different L_0 on the time when initial kinetic energy $E_{cm} = 324$ MeV.

Curve 5, if $L_0 = 80$, shows the decay of interacting nuclei, which have not overcome the Coulomb barrier; it also demonstrates the need to consider L_c in the calculation of the capture cross sections. Other curves show the entry of the system into the capture channel. With increase of L_0 the velocity of entry $(\partial E_{cm}/\partial R)$ into the capture channel is decreased; it is determined by the rate of the angular momentum change after the Coulomb barrier. This observation illustrates usefulness of condition (6).

It should be borne in mind, that condition (6) limits the dissipation of the kinetic energy into the excitation energy at the capture momentum. Then the system inertial momentum is equal to $\mu R^2 + j_1 + j_2$, where j_1 and j_2 - inertial momenta of light and heavy nuclei.

CAPTURE CROSS SECTION AND PROBABILITY

The expression averaged over all possible angular momenta L_{max} which were involved in the reaction [9] was used in order to calculate the capture cross section σ_{cap} for a fixed isotope configuration of interacting nuclei:

$$\sigma_c(E_{cm}) = \frac{\pi\hbar^2}{2\mu E_{cm}} \cdot \frac{1}{L_{max}(E_{cm})} \sum_{L_{0i}=0}^{L_c(E_{cm},L_{0i})} (2L_{0i}+1) P_i(E_{cm}, L_i), \quad (7)$$

where $P_i(E_{cm}, L_i)$ – capture probability, E_{cm} – kinetic energy, $\mu = m_1 \cdot m_2/(m_1+m_2)$ – reduced mass of nuclei, $L_c(E_{cm}, L_{0i})$ – critical (maximum) value of angular momentum, contributing to the capture cross section, L_{0i} – current value of angular momentum.

Maximum value of the angular momentum L_{max} can be easily obtained from the energy balance at contact points of interacting nuclei: $E_{cm} - V_n^{cont} - V_{Coul}^{cont} - V_{rot}^{cont} = \mu\dot{R}^2/2$, where V_{Coul}^{cont}, V_n^{cont} and V_{rot}^{cont} - Coulomb, nuclear and centrifugal potentials at the contact point. The angular momentum is defined as [7]: $|L| = \mu R \dot{R} \sin\theta$, where $R = R_1 + R_2$, $\dot{R}$ – velocity at the contact point, θ – angle between the axis of the beam and distances between centers of interacting nuclei, which is equal to $\pi/2$ for determination of the maximum value, thus:

$$L_{max} = \frac{\sqrt{2\mu R^2 (E_{cm} - V_{Coul} - V_n)(1-\hbar^2) + 2\hbar^4} - 0.5\hbar^2}{1+\hbar^2},$$

if $\hbar^2 \to 0$:

$$L_{max}(E_{cm}) = (R_1 + R_2) \cdot \sqrt{2\mu(E_{cm} - V_{Coul}^{cont} - V_n^{cont})}. \quad (8)$$

Verification of expression (8) was carried out in the reactions below and confirmed the correctness of the chosen assumption.

At the fixed kinetic energy of the beam and the initial angular momentum the capture probability is determined by [9]:

$$P_i(E_{cm}, L_i) = 1 - \exp\left(-\frac{E_{qf(i)}(L_i) - \Delta E_i^*(E_{cm}, L_i)}{\Theta_i(E_{cm}, L_i)}\right), \quad (9)$$

where $\Theta_i(E_{cm}, L_i) = \sqrt{12E_i^*(E_{cm}, L_i)/A_0}$ - temperature of nuclei after dissipation of the kinetic energy into the excitation energy $E_i^*(L_i)$. $E_{qf(i)}(L_i)$ – energy which is required to overcome the quasifission barrier and is determined from the interaction dynamics. $\Delta E_i^*(E_{cm}, L_i) = \left|E_{1(i)}^*(E_{cm}, L_i) - E_{2(i)}^*(E_{cm}, L_i)\right|$ – difference between the excitation energies of heavy and light nuclei. With regard to the fact that nucleons are not transferred from one nucleus to another and there is no emission of nucleons prior to the momentum of capture, the excitation energy is calculated in proportion to the mass numbers of interacting nuclei. It follows from the above expressions that capture cross section depends on the angular momentum in a complicated fashion.

Fig. 8 shows dependences of the capture probability for $^{50}Ti + ^{251}Cf$ reaction on the angular momentum which were calculated by means of (9) for various initial kinetic energies of the beam. The calculations showed that with the

increase of the kinetic energy, at first, the contribution of values of the angular momentum in the capture reaction is increased, and as E_{cm} is further increased, L value was reduced by the decrease of the energy required to overcome the quasifission barrier E_{qf}. The capture probability is close to 1 with a relatively small E_{cm}, but with energy which is sufficient to overcome the Coulomb barrier. With increase of E_{cm} the excitation energy is increased and E_{qf} is decreased, therefore, the capture probability is decreased. This process limits L_c values in reaction. Changes in the critical angular momentum for $^{46-50}Ti + ^{251}Cf$ reactions from the kinetic energy are shown in Fig. 9.

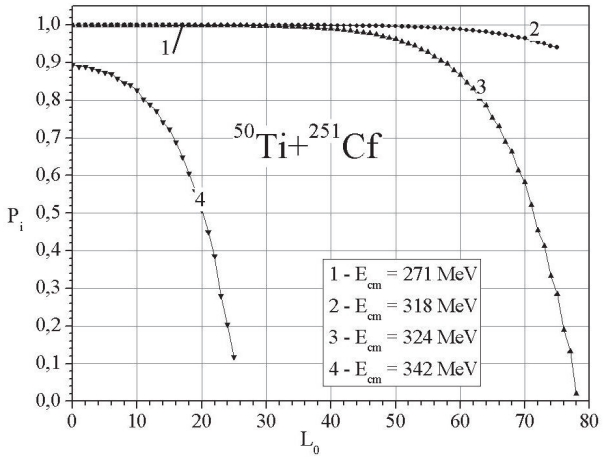

Fig. 8. Dependence of the capture probability on the angular momentum for different kinetic energy of the beam for $^{50}Ti + ^{251}Cf$ reaction.

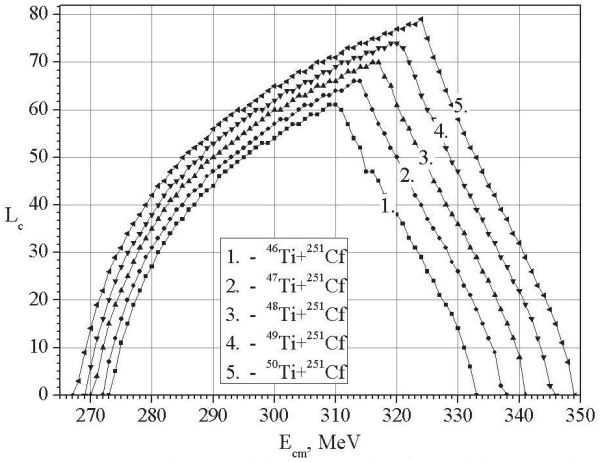

Fig. 9. Dependence of the critical value of the angular momentum on the kinetic energy.

It follows from the graphs that L_c is increased with increase of the kinetic energy due to overcoming the Coulomb barrier by nuclei with higher angular momenta. Maximum L_c is attained after the maximum value of the capture cross section. Then the excitation energy is increased and the capture probability is decreased to zero. While increasing E_{cm} the system temperature rises, but it does not bring significant contribution to the capture cross section. Such dependences were observed in all reactions.

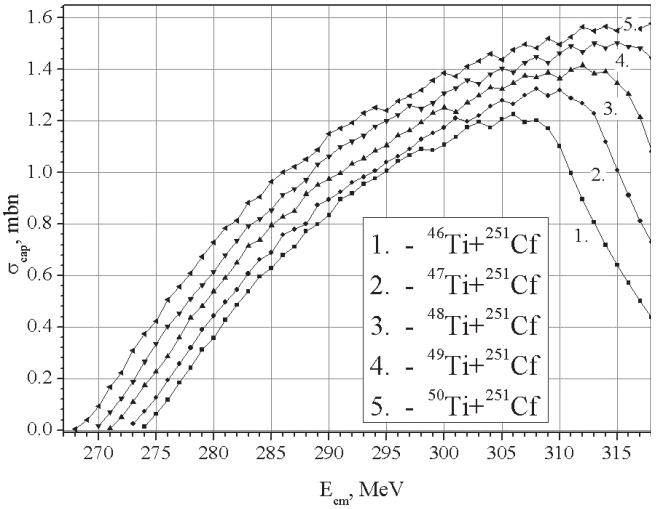

Fig. 10. Dependence of the capture cross section on the kinetic energy.

Since the increase of E_{cm} leads to the increase of the excitation energy which is removed from the compound nucleus by the emission of nucleons and γ-quants, thus reducing the probability of SHE formation, experimental works should be carried out at energies when $0 < \sigma_{cap} \le \sigma_{cap}^{max}$. Therefore, Fig. 10 shows the dependence of capture cross sections on the kinetic energy of the beam in the range of the capture cross section growth. With increase of the neutron number in the light nucleus the kinetic energy range is increased with increase of the capture cross section from zero to a maximum value.

Growth of curves with increase in the kinetic energy (Fig. 10) is due to the inclusion of higher values of the angular momenta which contribute to the reaction. In addition, the excitation energy difference is increased and, consequently, the capture probability is decreased (Fig. 4). Almost upon attainment of the maximum value, the capture probability falls due to the decrease of the quasifission barrier. As the initial angular momentum L_0 is increased, L_c values, contributing to the capture, are decreased and the system passes into the quasifission channel upon disappearance of the quasifission barrier, where σ_{cap} becomes zero.

RESULTS AND DISCUSSIONS

Probabilities (9) and capture cross section (7) have been calculated while solving system (4), from the contact of nuclei to the capture moment which is defined by expression (5). The results of these calculations are shown in Fig. 11, 12 and Table 1.

Calculations showed that the angular momentum has significant effect on the capture process. The increase of the

initial value of the angular momentum leads to the increase of the centrifugal potential and therefore, to the decrease of the quasifission barrier height. For example, for $^{54}Cr+^{248}Cm$ reaction with $L_0 = 0$ $B_{qf} = 4.21$ MeV, and with $L_0 = 70$ $B_{qf} = 0.02$ MeV. Consequently, the capture is impossible for angular momentum that exceeds a critical value.

Table 1.

Results of the calculations

Reaction	E_{cm} / E_{cm}^{avg}, MeV	L_{max}	L_{crit}^{max}	σ_{cap}^{max}, mbn	E^* / E_{avg}^*, MeV
$Z_1 + Z_2 = Z_0 = 120$					
$^{80}Ge+^{222}Rn$	366 – 371 / 368.5	189 – 196	25	0.1	67.75 – 71.98 / 69.87
$^{73}Ge+^{226}Ra$	355 – 362 / 358.5	177 – 185	30	0.14	65.34 – 71.59 / 68.47
$^{74}Ge+^{226}Ra$	354 – 364 / 359	183 – 195	37	0.19	64.5 – 73.58 / 69.04
$^{76}Ge+^{226}Ra$	350 – 366 / 358	179 – 199	48	0.325	61.86 – 76.58 / 69.22
$^{69}Ga+^{227}Ac$	329 – 349 / 339	149 – 174	49	0.425	47.43 – 62.59 / 55.01
$^{71}Ga+^{227}Ac$	329 – 351 / 340	142 – 174	57	0.61	45.44 – 65.48 / 55.46
$^{64}Zn+^{232}Th$	345 – 349 / 347	166 – 173	16	0.025	65.07 – 68.48 / 66.78
$^{66}Zn+^{232}Th$	341 – 350 / 345.5	168 – 177	29	0.15	62.15 – 68.98 / 65.57
$^{67}Zn+^{232}Th$	339 – 351 / 345	171 – 183	36	0.23	60.68 – 69.78 / 65.23
$^{68}Zn+^{232}Th$	338 – 353 / 345.5	166 – 185	44	0.31	60.21 – 73.27 / 66.74
$^{70}Zn+^{232}Th$	335 – 355 / 345	166 – 192	53	0.47	58.21 – 76.27 / 67.24
$^{63}Cu+^{231}Pa$	334 – 347 / 340.5	157 – 172	33	0.22	60.98 – 69.98 / 65.48
$^{65}Cu+^{231}Pa$	332 – 349 / 340.5	159 – 180	45	0.385	58.58 – 73.58 / 66.08
$^{58}Ni+^{238}U$ (1a)	332 – 336 / 334	157 – 162	21	0.09	62.1 – 67.36 / 64.73
$^{60}Ni+^{238}U$ (1b)	329 – 339 / 334	161 – 173	36	0.235	60.23 – 69.5 / 64.87
$^{61}Ni+^{238}U$ (1c)	327 – 339 / 333	159 – 173	41	0.33	59.6 – 69.98 / 64.79
$^{62}Ni+^{238}U$ (1d)	327 – 342 / 334.5	159 – 177	50	0.44	58.19 – 72.42 / 65.31
$^{64}Ni+^{238}U$ (1e)	323 – 343 / 333	160 – 186	57	0.62	53.93 – 74.96 / 64.45
$^{59}Co+^{237}Np$	319 – 336 / 327.5	151 – 173	51	0.529	55.2 – 72.27 / 63.74
$^{54}Fe+^{244}Pu$ (2a)	313 – 324 / 318.5	144 – 158	39	0.405	56.07 – 66.25 / 61.16
$^{56}Fe+^{244}Pu$ (2b)	309 – 328 / 318.5	142 – 166	51	0.624	53.6 – 71.55 / 62.58
$^{57}Fe+^{244}Pu$ (2c)	307 – 324 / 315.5	142 – 163	48	0.71	51.74 – 67.84 / 59.79
$^{58}Fe+^{244}Pu$ (2d)	308 – 331 / 319.5	148 – 177	60	0.82	52.41 – 74.44 / 63.43
$^{55}Mn+^{243}Am$	297 – 326 / 311.5	136 – 173	59	0.892	48.73 – 76.25 / 62.49
$^{50}Cr+^{248}Cm$ (3a)	292 – 315 / 303.5	127 – 156	51	0.797	48.46 – 70.94 / 59.7
$^{52}Cr+^{248}Cm$ (3b)	289 – 319 / 304	130 – 165	62	1.021	46.59 – 76.03 / 61.31
$^{53}Cr+^{248}Cm$ (3c)	288 – 323 / 305.5	130 – 174	65	1.092	45.78 – 79.83 / 62.81
$^{54}Cr+^{248}Cm$ (3d)	286 – 325 / 305.5	128 – 179	69	1.178	44.68 – 82.83 / 63.76
$^{50}V+^{247}Bk$	280 – 318 / 299	122 – 168	65	1.2	44.06 – 81.14 / 62.6
$^{51}V+^{247}Bk$	278 – 320 / 299	121 – 173	69	1.3	42.61 – 84.24 / 63.43
$^{46}Ti+^{251}Cf$ (4a)	274 – 305 / 289.5	116 – 154	58	1.24	43.56 – 74.62 / 59.09
$^{47}Ti+^{251}Cf$ (4b)	273 – 310 / 291.5	120 – 163	64	1.35	42.69 – 79.82 / 61.26
$^{48}Ti+^{251}Cf$ (4c)	271 – 312 / 291.5	120 – 169	68	1.4	41.49 – 82.53 / 62.01
$^{49}Ti+^{251}Cf$ (4d)	270 – 315 / 292.5	121 – 174	72	1.5	40.84 – 85.93 / 63.39
$^{50}Ti+^{251}Cf$ (4e)	268 – 318 / 293	121 – 180	76	1.59	39.6 – 89.62 / 64.61
$^{45}Sc+^{252}Es$	262 – 306 / 284	113 – 161	67	1.583	40.19 – 83.32 / 61.76
$^{48}Ca+^{257}Fm$	245 – 298 / 271.5	111 – 173	82	2.13	33.36 – 86.8 / 60.08
$Z_0 = 126$					
$^{70}Zn+^{247}Cm$	360 – 363 / 361.5	185 – 187	16	0.033	66.5 – 68.56 / 67.53
$^{62}Ni+^{251}Cf$	346 – 350 / 348	166 – 169	17	0.03	65.4 – 68.24 / 66.82
$^{64}Ni+^{251}Cf$	343 – 351 / 347	169 – 179	31	0.17	64.36 – 68.87 / 66.62
$^{59}Co+^{254}Es$	339 – 343 / 341	163 – 166	21	0.08	62.88 – 65.95 / 64.42
$^{56}Fe+^{257}Fm$	328 – 335 / 331.5	153 – 162	26	0.15	58.5 – 65.14 / 61.82
$^{57}Fe+^{257}Fm$	327 – 337 / 332	158 – 171	35	0.245	58.08 – 67.34 / 62.71
$^{58}Fe+^{257}Fm$	326 – 340 / 333	155 – 169	41	0.35	56.24 – 69.24 / 62.74
$^{55}Mn+^{260}Md$	316 – 331 / 323.5	148 – 166	43	0.46	54.37 – 68.43 / 61.4

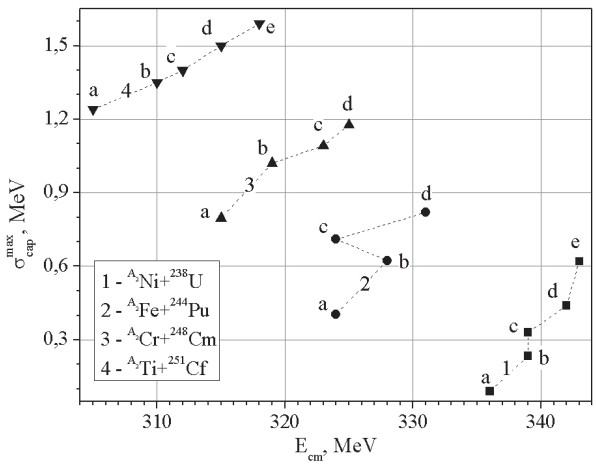

Fig. 11. Dependence of the maximum value of the capture cross section on the initial kinetic energy for perspective reactions of SHE with $Z_0 = 120$. Reactions shown in the graph are specified in the Table 1.

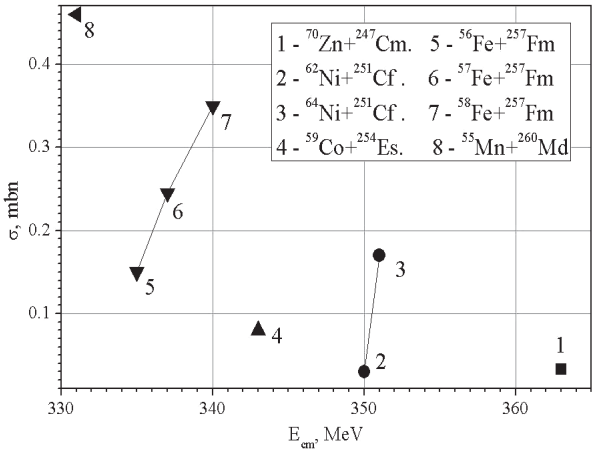

Fig. 12. Dependence of the maximum value of the capture cross section on the initial kinetic energy for some reactions of SHE with $Z_0 = 126$.

Calculations of the dynamics of interacting nuclei showed that the value of the angular momentum is reduced to 30% of the initial value, and therefore there is a potential well in the interaction potential, while it is absent at the momentum of contact. This means that greater number of the angular momenta contributes to the reaction. For example, the critical value for ^{48}Ca+^{257}Fm reaction is 68, but the value amounting to 82 takes part in the reaction.

In case of the isotope configuration it follows from the obtained data that it is appropriate to use elements with high charge asymmetry and neutron-rich light nuclei. The charge asymmetry has an influence due to the fact that the Coulomb potential is reduced with increase of the asymmetry and accordingly the Coulomb barrier is decreased. For example, for ^{80}Ge+^{222}Rn reaction which has $\eta_Z = 0.43$, $L^{max}_{crit} = 25$, $\sigma^{max}_{cap} = 0.1$ mbn and for ^{48}Ca+^{257}Fm reaction – $\eta_Z = 0.67$, $L^{max}_{crit} = 82$, $\sigma^{max}_{cap} = 2.13$ mbn. With decrease of mass asymmetry, where $\eta_Z = Const$, the nuclear potential is increased, and, therefore, the height of quasifission barrier is increased. For example, for ^{47}Ti+^{251}Cf reaction with $\eta_A = 0.68$, $L^{max}_{crit} = 64$, $\sigma^{max}_{cap} = 1.24$ mbn and for ^{50}Ti+^{251}Cf reaction – $\eta_A = 0.67$, $L^{max}_{crit} = 76$, $\sigma^{max}_{cap} = 1.59$ mbn.

Number of the angular momenta due to which light nucleus overcomes the Coulomb barrier is increased with increase of the kinetic energy, as well as the critical value of angular momentum is increased. This leads to increase of the excitation energy and therefore, to the decrease of the capture probability. That is to say that smaller number of angular momenta contributes to the capture process and the capture cross section decreases. Therefore, it is appropriate to carry out experimental works at energies when $0 < \sigma_{cap} < \sigma^{max}_{cap}$.

Increase of the compound nucleus charge reduces the capture cross section and the critical angular momentum, while the kinetic energy and the excitation energy is increased. For example in ^{55}Mn+^{260}Md→^{315}126 reaction these parameters are $\sigma^{max}_{cap} = 0.46$ mbn, $L^{max}_{crit} = 43$, $E^{avg}_{cm} = 323.5$ MeV, $E^{*}_{avg} = 54.37$ MeV. For ^{54}Cr+^{248}Cm→^{302}120 reaction these parameters are $\sigma^{max}_{cap} = 1.178$ mbn, $L^{max}_{crit} = 69$, $E^{avg}_{cm} = 305.5$ MeV, $E^{*}_{min} = 44.68$ MeV. In addition the parameters of mass and charge asymmetry are the same for the above reactions.

CONCLUSIONS

Effect of the angular momentum on the capture cross section and the excitation energy is shown on the basis of the dynamic-statistical description of the capture process in fusion-quasifission reactions of heavy nuclei. Based on this description, it became possible to determine the stability region where the capture and thus the SHE formation are possible. Consequently, effect of the angular momentum on isotope configuration of a target beam and on the collision kinetic energy should be taken into consideration during the planning of experiments.

REFERENCES

1. Oganessian Yu.Ts., Dmitriev S.N. Superheavy elements of D.I. Mendeleev periodical system // Successes of Chemistry**.** – 2009. – Vol. 78. – P. 1165-1176. (in Russian).
2. Oganessian Yu. Ts., Abdullin F. Sh., Bailey P. D. et al. Synthesis of a New Element with Atomic Number Z = 117 // Phys. Rev. Let. – 2010. – Vol. 104. – P. 142502.
3. Hoffman Z. Synthesis of superheavy elements by the method of cold fusion // Successes of Chemistry**. –** 2009. – Vol. 78. – P. 1211-1227. (in Russian).
4. Bomko V.A., Zaytsev B.V., Kobets A.F. et al. Accelerating structures of before grinding section of heavy ion linear accelerator LUMZI // QAST. – 2012. – Vol. 80. – P. 20-23. (in Russian).
5. Zaytsev B.V., Tishkin S.S., Shulika N.G. As the use of a combination of highfrequency focus in high-current heavy ion linear

accelerators // QAST. – 2010. – Vol. 54. – P. 85-89. (in Russian).
6. Volkov V.V. Process of Complete Fusion of Atomic Nuclei. Complete Fusion of Nuclei in the Framework of the Dinuclear System Concept // PEPAN. – 2004. – Vol. 35. – P. 798-857. (in Russian).
7. Fazio G., Giardian G., Nasirov A.K. et al. Formation of heavy and superheavy elements by reactions with massive nuclei // Eur. Phys. J. A. – 2004. – Vol. 19. – P. 89-104.
8. Myers W.D., Swiatecki W.J. Nucleus-nucleus proximity potential and superheavy nuclei // Phys. Rev. C. – 2000. – Vol. 62. – P. 044610.
9. Anokhin R.A., Pavlii K.V. Dynamic-statistical description of capture cross-section - initial stage of the fusion of heavy nuclei reactions // QAST. – 2011. – Vol. 56. – P. 16-23.

Pavlii Konstantin Vsevolodovich - National scientific center “Kharkov institute of physics and technology”, senior scientist, candidate of physics-mathematics sciences.
Science area: fusion-quasifission reactions of heavy nuclei, fission of nuclei, accelerators, radiation damage physics

Anokhin Roman Aleksandrovich - National scientific center “Kharkov institute of physics and technology”, research engineer.
Science area: fusion-quasifission reactions of heavy nuclei, fission of nuclei, astrophysics, artificial intellect